Hydrological Sciences Journal

ISSN: 0262-6667 (Print) 2150-3435 (Online) Journal homepage: www.tandfonline.com/journals/thsj20

Assessment of hydropedological characteristics at medium-sized landslide sites in Manafwa catchment, Mount Elgon, Uganda

Moses Kutosi, Yazidhi Bamutaze, Bob R. Nakileza, Yeeko Kisira & Geofrey Gabiri

To cite this article: Moses Kutosi, Yazidhi Bamutaze, Bob R. Nakileza, Yeeko Kisira & Geofrey Gabiri (2024) Assessment of hydropedological characteristics at medium-sized landslide sites in Manafwa catchment, Mount Elgon, Uganda, Hydrological Sciences Journal, 69:10, 1249-1260, DOI: 10.1080/02626667.2024.2366351

To link to this article: https://doi.org/10.1080/02626667.2024.2366351

Published online: 08 Jul 2024.

Submit your article to this journal

Article views: 196

View related articles

View Crossmark data

Citing articles: 1 View citing articles

Full Terms & Conditions of access and use can be found at
https://www.tandfonline.com/action/journalInformation?journalCode=thsj20

HYDROLOGICAL SCIENCES JOURNAL
2024, VOL. 69, NO. 10, 1249–1260
https://doi.org/10.1080/02626667.2024.2366351

Check for updates

Assessment of hydropedological characteristics at medium-sized landslide sites in Manafwa catchment, Mount Elgon, Uganda

Moses Kutosi [a], Yazidhi Bamutaze [b], Bob R. Nakileza [c], Yeeko Kisira [d] and Geofrey Gabiri [e]

[a]Department of Environment and Social Safeguards, Uganda National Roads Authority (UNRA), Kampala, Uganda; [b]Geography, Geo-Informatics and Climatic Sciences, Makerere University, Kampala, Uganda; [c]Department of Environmental Management, Makerere University, Kampala, Uganda; [d]Department of Geography, Gulu University, Gulu City, Uganda; [e]Department of Geography and Social Studies, Kyambogo University, Kampala, Uganda

ABSTRACT

Though strongly linked to landslides, hydropedological characteristics are inadequately investigated in Manafwa catchment. This study investigated hydropedological characteristics at medium landslide sites in Manafwa catchment. The design included 12 infiltration experiments that were conducted at each site. To determine the selected soil physical properties, composite soil samples were extracted from the infiltration sites for soil laboratory analysis. Soil cores were extracted to determine saturated hydraulic conductivity (Ksat) and bulk density. The observed high infiltration rates and rapid Ksat underscore the susceptibility of the studied sites to landslide hazards. Additionally, soil organic matter, clay content, and bulk density further contribute to the understanding of the hydropedological factors influencing landslide occurrences. These findings reveal the need for comprehensive investigations into hydropedological characteristics of other landslide categories to assist in landslide risk assessment and management strategies.

ARTICLE HISTORY
Received 9 May 2023
Accepted 17 May 2024

EDITOR
K. Soulis

ASSOCIATE EDITOR
(not assigned)

KEYWORDS
Infiltration rate; saturated hydraulic conductivity; soil properties; medium landslides; Manafwa catchment; Uganda

1 Introduction

Landslide hazards are prevalent in highland environments and have been described as one of the most damaging natural hazards (Guzzetti *et al.* 2012, Broeckx *et al.* 2018). Globally, landslide hazards are reported to be on the increase due to the increasing climate change extremes such as heavy rainfall, coupled with human activities. Notably, most damages and fatalities from landslides occur in the Global South, particularly in the Himalayan arc of Asia (Petley 2012, Broeckx *et al.* 2018). Also, on the African continent, the last 20 years have witnessed an increase in landslides, with the East African highland areas being the hotspot for these hazards (Kervyn *et al.* 2015, Bamutaze 2019). Despite the increasing landslide hazards and the associated adverse impacts, studies addressing them, especially in equatorial Africa, are still scanty, particularly in terms of characterization of hydrological and pedologic factors that underpin landslide occurrence.

The available literature indicates that hydrological conditions significantly influence landslide occurrences (Travelletti *et al.* 2011, Bogaard and Greco 2014, Bicocchi *et al.* 2019, Wayllace *et al.* 2019). In particular, infiltration and hydraulic conductivity are the dominant hydrological soil properties that trigger landslides on hill slopes (Aristizábal *et al.* 2016, Chienyuan and Tien-chien 2017). Dynamics in the infiltration process may cause secondary soil creep and debris flow within a landslide scar (Chien-yuan and Tien-chien 2017). Water in the unsaturated soil surfaces leads to reduced shear strength of the soil, thereby increasing the possibility of slope failure.

Hydraulic conductivity triggers landslides in mountainous areas with more permeable and deeper soils. Soils of high conductivity only require short and intense rainfall for failure to occur (Aristizábal *et al.* 2016). In tropical mountainous environments, there are high rainfall amounts and deep weathering profiles in saturated or humid field conditions. This is why shallow landslides triggered by rainfall in tropical environments are controlled by the volume of water infiltrating the soil. Therefore, understanding the soil characteristics of steady-state infiltration rate and saturated hydraulic conductivity is very important in landslide assessment and management (Hiramatsu *et al.* 1993, Chiu *et al.* 2019).

Manafwa catchment has experienced several landslides, but knowledge of the influence of hydrological parameters on the occurrence of landslides is still limited. And yet, such knowledge is critical for monitoring and mitigation strategies for landslides. Rainwater tends to infiltrate into the slope materials, and as a result, these materials are rendered unstable (Yeh and Tsai 2018). This explains why the catchment experienced one of the largest landslides in March 2010, leading to the deaths of over 300 people (Mugagga *et al.* 2012a, Osuret *et al.* 2016, Nakileza *et al.* 2017). In addition, another deadly landslide occurred in 2018, which claimed over 50 lives and caused displacement of 858 people (Acaps 2018). All these deadly landslides have been experienced after heavy downpours. A study by Broeckx *et al.* (2018) underscored the limited information available regarding the soil hydrological parameters that underpin landslides in this area.

CONTACT Moses Kutosi kutosimoses04@gmail.com Department of Environment and Social Safeguards, Uganda National Roads Authority (UNRA), Plot 3-5 New Port Bell Road, UAP Nakawa Business Park, P.O. Box 28487, Kampala, Uganda

© 2024 IAHS

This has resulted in constrained early warning and risk management. Cognizant of this existing gap, the gist of this study was to assess the hydropedological conditions underpinning landslide occurrence, with a special focus on the medium landslides as defined by Singh *et al.* (2008) in Manafwa catchment, Mount Elgon. The study assessed the variation of soil physical properties between the sampled landslide scar sites in the catchment and intrinsic variations of the same within the landslide scars (between sections). The study also determined the steady-state infiltration rates and hydraulic conductivity between the studied landslide scar sites across the catchment and within the landslide scars. It also assessed the influence of selected physical soil properties on infiltration and hydraulic conductivity in the catchment.

2 Materials and methods

2.1 The study area

The study was conducted in the Manafwa catchment located between 34°7′30” and 34°30′0”E and between 0°52′30” and 1° 7′30”N on Mount Elgon in Eastern Uganda (Fig. 1). This area experiences more severe major landslides than other landslide-prone areas in the country (Kisira *et al.* 2022). Its altitude ranges from 1104 to 4139 m above sea level. Manafwa River is the main river in the catchment and also one of the five main rivers draining the Mount Elgon landscape into the Lake Kyoga basin (Wodeya 2018, Bamutaze 2019).

The area receives annual rainfall within a range of 1200 to 1600 mm (Wodeya 2018, Bamutaze 2019, Nakileza and Nedala 2020). This characterizes the catchment as a high rainfall receiving area, which positively correlates with frequent occurrence of landslides. Landslides that follow the dry season are said to occur after the first rains infiltrating very fast into the open cracks causing rapid volume change and triggering landslides (Kitutu 2010). The area has two distinct seasons, with the wettest period occurring from April to October. The minimum and maximum temperatures of the area are 15 and 23° C respectively (Mugagga *et al.* 2012b).

Mount Elgon is associated with volcanoes and is the oldest of the solitary extinct volcano in East Africa that rests on the dissected peneplain of the Precambrian bedrock of the Trans-Nzoia plateau (Precambrian basement complex) (Tamale 2014). The geology is dominated by fenitized basement, agglomerates, and tuffs. Kitutu (2010) found that fenitized basements and phonolite dykes are prone to landslides. The relatively young and fertile calcium-, sodium-, and potassium-rich soils that cover the slopes are moist, dark humus loams. On the steep slopes in the high-altitude moorlands, very shallow soils are found, while red-brown clay loams have formed on the gentle slopes (Mugagga *et al.* 2012a). With stand-alone volcanic cones, interlocking spurs, V-shaped valleys, and

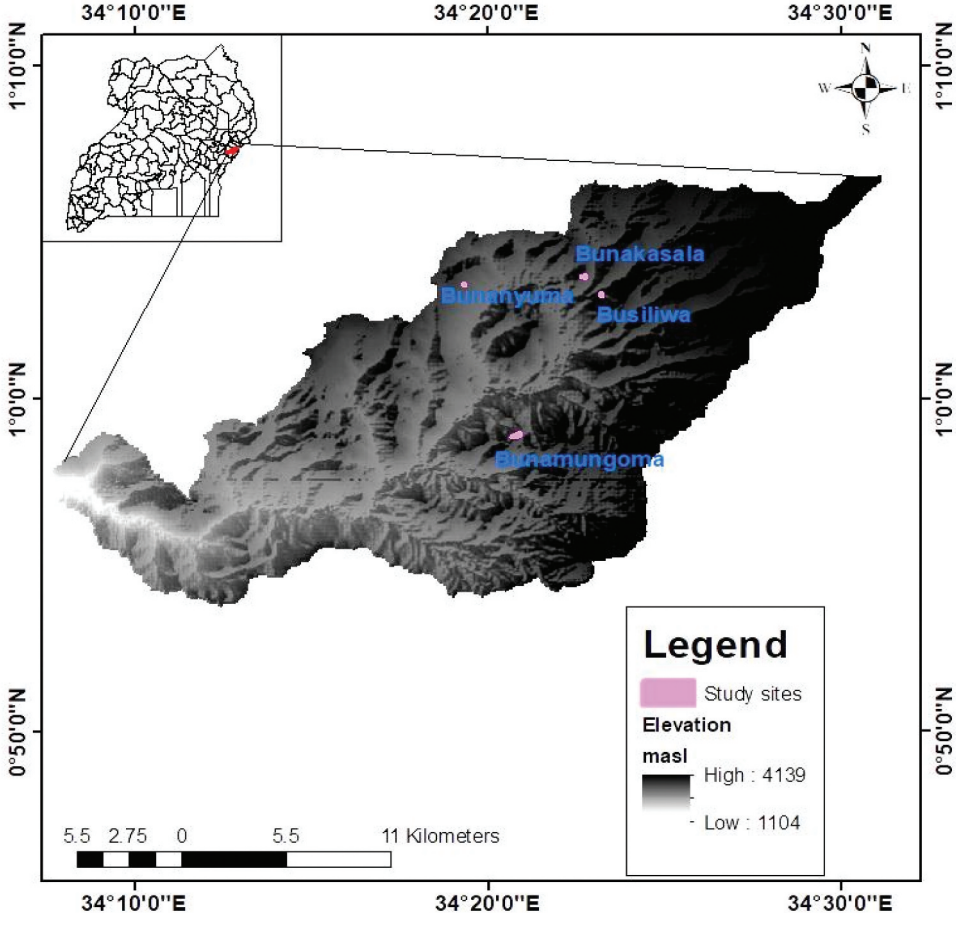

Figure 1. Location of the catchment study area in Uganda and distribution of the studied sites in the catchment.

ridges both gently undulating and rugged, the catchment is hilly to the northeast and relatively flat to the southwest (Fig. 1).

2.2 Mapping of landslide scars

First, reconnaissance was conducted in the study area as shown in Fig. 2. The reconnaissance entailed consultations with the environmental officers and disaster focal persons in Bududa and Manafwa districts to identify major landslides that had occurred to date in the area and were recorded at the district level. These consultative meetings provided information on the sites/locations where landslides had previously occurred, including the dates. This information also guided the research team while visiting these sites to take note of measurements for site characteristics. At each identified landslide site, the length and width were recorded using a tape measure to enable computation of the area/size of the landslide. In addition, the coordinates and altitude at the landslide site were recorded using a global positioning system (GPS, Garmin 60sx). During this phase, an inventory was developed of landslide hazards that had occurred in the catchment, and their sizes were computed (Table 1). The major landslides identified during the reconnaissance phase were then classified by size following the procedure of Singh *et al.* (2008). The major landslides in the catchment belong to the medium-sized landslides class (Table 2).

2.3 Research design

Given that the majority of the mapped landslide scars were medium landslides ranging from 1000 to 100 000 m^2, as categorized by Singh *et al.* (2008), four of these scars were selected for the study as depicted in the landslide inventory in Table 1. The study then applied an experimental design including a randomized block design (RBD). The blocks (landslide scars) consisted of three landslide scar sections: the head scarp, main body, and deposition (see Fig. 3). In each section, four infiltration measurements (replicates) were conducted, two on each side (left and right) of the three landslide scar sections across the four selected sites in the study area. Twelve experiments were run at each study site (landslide scar), making a total of 48 infiltration experiments.

2.4 Sampling to determine soil physical properties at landslide sites

Soil samples were collected at different depths of topsoil (0–15 cm) and subsoil (15–30 cm) within a radius of 2 m at three different points around each infiltration experimental site. The samples were mixed thoroughly in a bucket, and a portion (composite sample) for each soil depth was taken to the laboratory for analysis of soil physical properties following standard methods (Okalebo *et al.* 2002). A total of 96 composite soil samples were collected, i.e. 48 samples for each depth. Composite soil sampling at various depths is a crucial practice in rigorous soil analysis since it reveals substantial vertical variability of factors such as organic matter content, nutrient distribution, and soil texture (Dick *et al.* 2015, Yimer *et al.* 2015, James and Wells 2018). Furthermore, Perkins *et al.* (2013) emphasized that composite samples can be considered during rigorous soil sample analysis, especially when a plot is the unit of study, taking vegetation biomass and nutrient

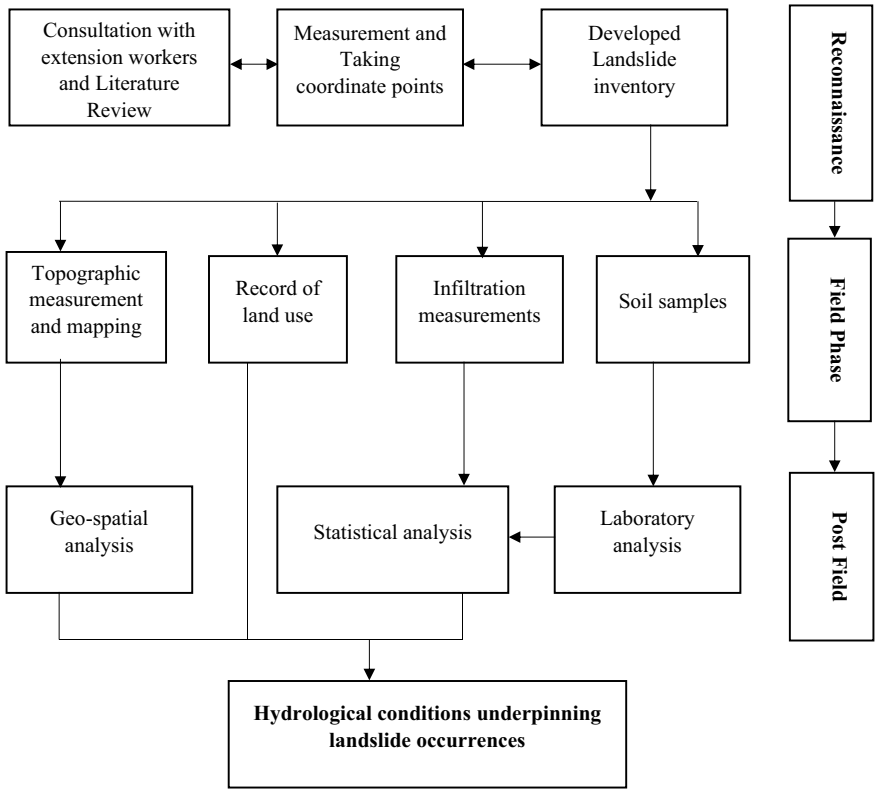

Figure 2. Methodological framework for the study.

Table 1. Inventory of identified medium-sized landslide scars.

ID	X	Y	Altitude (m)	Year of occurrence	Slope (°)	Thickness by Length (m)	Thickness by width (m)	Area (m^2)
1	654 725	111 736	1840	2019	38	757	50	37 850
2	649 591	117 992	1683	2019	18	146	67	9782
3	655 556	110 967	1556	2019	24	115	43	4945
4	653 718	111 100	1371	2019	28	82	58	4756
5	649 930	117 970	1644	2019	26	105	39	4116
6	649 873	118 056	1648	2019	30	96	32	3072
7	649 311	118 046	1621	2019	25	73	21	1533
8	650 062	108 607	1515	2018	25	182	86	15 652
9	647 771	116 987	1602	2018	21	77	49	3773
10	647 644	116 462	1534	2018	14	25	83	2075
11	655 393	114 520	1743	2018	34	55	35	1925
12	654 626	115 018	1767	2017	27	73	40	2920
13	649 345	117 587	1510	2015	17	315	73	22 995
14	647 018	116 960	1731	2015	26	150	45	6750
15	655 012	114 526	1714	2015	30	90	42	3780
16	647 404	116 731	1622	2015	25	85	43	3655
17	647 234	117 198	1750	2015	29	58	46	2668
18	653 495	117 306	1677	2012	22	220	80	17 600
19	654 240	116 417	1590	2012	30	140	35	4900
20	650 196	117 840	1531	2012	24	60	25	1500
21	650 198	177 816	1522	2010	23	56	34	1904
22	648 918	107 354	1520	1998	26	85	35	2975
23	655 501	114 924	1790	1998	32	69	37	2553
24	648 705	108 109	1455	1997	25	105	87	9135
25	649 265	108 290	1456	1997	30	127	45	5715
26	648 140	117 280	1569	1997	27	79	45	3555
27	653 839	116 738	1483	1997	22	83	27	2241

Table 2. Landslide classification.

Size (m^2)	Description based on size
<10	Very small
10–1000	Small
1000–100 000	Medium
100 000–1 000 000	Large
>1 000 000	Very large

Source: Singh *et al.* (2008).

content expressed on a plot basis as it reduces cost and analytical time. The use of composite samples also presupposes that a reliable mean estimate for a soil property can be derived from a solitary analysis of the composite sample. Therefore, this method is particularly suitable when the sampling area is recognized to exhibit a relatively consistent uniformity (Dick *et al.* 2015). Also, to capture this variability comprehensively, sampling at multiple depths was essential. The analysis of different depths allows for a more thorough assessment of the root zone. As various crops or plants have distinct root depths and nutrient uptake patterns, sampling at different depths provides valuable insights into nutrient availability within the critical root zone, aiding in effective crop management (Zhang *et al.* 2020).

The composite soil samples were taken to Makerere University Soil Science Laboratory for analysis following the standard soil analysis procedures presented by Okalebo *et al.* (2002). The results were used in the explanation of the observed hydrological properties in the catchment using a correlational statistical analysis. Also, bulk density was determined based on 48 samples that were extracted at each infiltration point for soil hydraulic conductivity following standard procedures. The results of soil properties were interpreted in relation to the critical levels. In soil analysis, the term "critical level" refers to the minimum concentration or content of a specific soil property in the soil below which a landslide trigger is not expected when soil organic matter is below the threshold level recommended for a given type of soil Zhang *et al.* (2023). In this study, the critical levels for the selected soil properties depict soil composition below or beyond which soil shear strengths decrease significantly to trigger landslides for the clay loam soils, as advanced by scholars elsewhere. Currently, many scholars interpret soil properties using critical levels of soil nutrients and properties; for example, Dörner *et al.* (2022) used critical values for different soil properties in andosols. Also, Samara *et al.* (2017) presented the effects of steel on soil using critical levels.

2.5 Determining the steady state infiltration rates

Soil infiltration in volcanic deep weathered soils creates conditions that trigger landslides. This has been proven by several studies around the world (Cho 2014, 2017, Galeandro *et al.* 2014, Guo and Ma 2023, Zhang *et al.* 2023). The infiltration of water increases soil moisture, reduces shear strength, and elevates pore pressure, making the soil mass more vulnerable to slope failure. In addition, the work by Qin *et al.* (2022) on the presence of shallow landslides induced by heightened hydraulic conductivity as a result of tree roots underscored the role of hydraulic conductivity with slope stability. Furthermore, work by Lora *et al.* (2016), who investigated infiltration dynamics in a physical hillslope model leading to shallow landslides triggered by rainfall, further evidenced the significant role of water infiltration in triggering landslides. Understanding these processes is crucial for assessing landslide risk in volcanic terrains and implementing effective mitigation measures in the catchment of Manafwa.

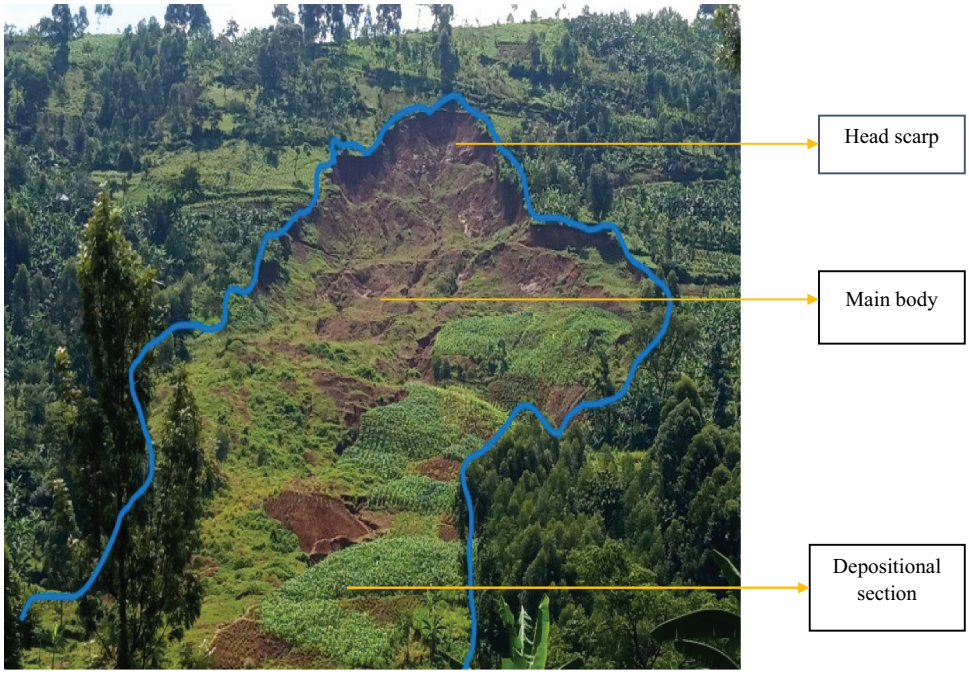

Figure 3. Landslide scar sections.

2.6 Layout of infiltration experiments

A double-ring infiltrometer was used to determine the infiltration at the study sites following standard procedures (Bouwer 1986) – see Fig. 4. The double-ring technique was adopted since it reduces the effect of slacking and lateral water flow (Bamutaze *et al.* 2010). A suitable position was selected within 1–2 m of the edge of each landslide scar (see blue line in Fig. 3). The inner ring was placed on the ground with the sharp edge facing down. A driving plate was then placed on top of the ring and driven 14 cm into the ground. The outer ring was then placed around the inner ring and driven to the same height as the inner ring while maintaining a vertical position for both rings. A 30 cm rule was placed vertically into the inner ring and supported by a string to avoid any displacement. The rings were continuously filled, keeping a water head of 9 cm in the inner ring and water level in the outer ring constant. Readings of water level in the inner ring were taken at various intervals of 1 to 5 and 10 min depending on the intake characteristics of the experiment site. The water in the inner ring was replaced after every complete experiment and reading. This was repeated until a constant value, referred to as the steady-state infiltration rate, was obtained three consecutive times.

2.7 Determining the hydraulic conductivity

A soil core was driven into the soil to obtain a soil sample at each infiltration experiment site after clearing twigs, grass, and stones. The core was then coded and taken to the laboratory to determine the soil's hydraulic conductivity. A total of 48 soil samples were collected. To determine the hydraulic the constant head method standard procedures (Amoozegar and Wilson 1999) were used.

Figure 4. Authors setting up the infiltration experiments in the field (2020).

2.8 Statistical data analysis

Quantitative analysis methods were used to analyse the data on infiltration, saturated hydraulic conductivity, and soil properties. For example, descriptive statistics was used to obtain the averages and level of variation. In addition, one-way analysis of variance (ANOVA) was used to analyse the variation of steady-state infiltration rates and saturated hydraulic conductivity. Regression analysis was used to determine the relationship between steady-state infiltration rates, saturated hydraulic conductivity, and soil physical properties.

3 Results

3.1 Variation of physical soil properties across the studied landslide sites

A summary of soil physical property data across soil depth is presented in Table 3. The soil organic matter is below the critical level of 3% as classified by Okalebo *et al.* (2002). Although increased infiltration and low soil water holding capacity were expected, the rapid infiltration caused fast filling of the soil pores, thus increasing pore pressure and hence increasing the chances of slope failure (Huang *et al.* 2022, Tian *et al.* 2022, Duan *et al.* 2023). In addition, soil organic matter, sand, and clay significantly varied with soil depth ($P < 0.05$) where soils at depths between 0 and 15 cm had the highest levels of organic matter (2.4%). The high clay content in the soil indicates they are extremely expansive hence increasing slope susceptibility to landslides. Soils with low organic matter at a depth of 15 to 30 cm provide a poor habitat for soil biota, such as earthworms. Such organisms, through their burrowing activities, increase pore space and create continuous pore linkage of surface to subsurface soil layers. The detected difference in clay with soil depth, therefore, explains the highly expansive soils that are associated with slope instability.

In addition, soils in the studied sites had low levels of bulk density, with a mean value of 1.26 g/cm^3 (Table 4). This is lower than the critical level (1.6 g/cm^3) for clay loam soils beyond which soil penetration is severely restricted, as emphasized by Hazelton and Murphy (2007). Low bulk density is associated with an increase in Ksat and infiltration rate which increases slope susceptibility to downslope movement.

3.2 Effect of soil physical properties on measured hydrological processes at the medium landslides

Results for the effect of physical soil properties on steady-state infiltration rates and saturated hydraulic conductivity at the four studied landslide scar sites are presented in Table 5. The soil organic matter increased with an increase in saturated hydraulic conductivity. This implied that soil organic matter, as opposed to soil texture, is a better predictor of soil hydraulic conductivity at landslide scars.

3.3 Variation of measured hydrological process at the medium landslides in the catchment

3.3.1 Steady-state infiltration rate between the studied landslide scars

The measured infiltration rates at the four landslide scar sites are presented in Table 6. The steady-state infiltration rate across the studied area varied from 0.03 to 1.22 cm/min with a range of 1.19 cm/min. A coefficient of variation of 63% was recorded, which is high according to the Coefficient of variation (CV) grouping by Couto *et al.* (2017). An average steady-state infiltration rate of 0.5 cm/min was recorded. Notably, the infiltration rate recorded was higher than the maximum basic infiltration rate of 0.016 cm/min for clay loams as classified by Brouwer *et al.* (1988). High steady-state infiltration rates and clay soils, which are known to reduce this rate, promote slope failure.

3.3.2 Steady-state infiltration rates within the landslide scars

Figure 5 summarizes the results of variation in the steady-state infiltration rate with landslide scar sections. In the entire catchment, the head scarp recorded the highest average steady-state infiltration rate of 0.5 cm/min, followed by the deposition section with 0.47 cm/min. The

Table 4. Variation of bulk density (0–15 cm).

Statistics	Bulk density (g/cm^3)
Average	1.26
CV (%)	8.24
Max	1.47
Min	1.01
Standard deviation	0.10

Table 3. Variation of soil properties with depth.

		% composition textural class				
Soil depth	Statistics	SOM	Sand	Clay	Silt	
0–15 cm	Average	2.4	34.6	35.3	30.1	
	CV (%)	30.9	17.5	14.5	15.3	
	Max	3.6	48	48	40	Clay loam
	Min	1.5	17.5	14.5	15.3	
	Standard deviation	0.7	6.1	5.1	4.6	
15–30 cm	Average	2	31.5	39.8	28.7	Clay
	CV (%)	26.4	19.1	14.2	15.2	
	Max	3	48	50	38	
	Min	1	18	14.2	15.2	
	Standard deviation	0.5	6	5.6	4.4	
ANOVA	F	15.0771	6.581	19.963	3.642	
	F crit	3.942	3.9423	3.9423	3.942	
	P value	0.000*	0.012*	0.000*	0.059	

*Significant difference (*P* value < 0.05); the more the ANOVA F > F crit the more the variation; Max = maximum; Min = minimum.

Table 5. Effect of physical properties on the measured hydrological processes.

		Physical properties			
Parameter	Statistics	SOM	Sand	Clay	Silt
IR	R^2	0.013	0.003	0.005	2.8×10^{-5}
	P value	0.43	0.71	0.63	0.97
Ksat	R^2	0.092	0.009	0.003	0.034
	P value	0.04*	0.52	0.71	0.21

*Significant R^2 ($P < 0.05$); R^2 = coefficient of determination.

Table 6. Measured IRs and Ksat rates with observed physiographic characteristics at the studied sites.

Scar sites	Sections	Replicate	X	Y	Land cover and use	Slope (%)	Altitude (m)	IR (cm/min)	Ksat (cm/min)
Bunamungoma	Head scarp	1	650 066	108 596	Coffee	50	1517	0.46	0.53
		2	650 052	108 587	Coffee	40	1502	1.08	1.32
		3	650 034	108 640	Abandoned	55	1516	0.34	0.83
		4	650 023	108 631	Abandoned	60	1497	0.34	1.03
	Main body	5	650 003	108 640	Cassava	48	1488	0.04	1.24
		6	649 982	108 630	Maize	45	1474	0.48	1.17
		7	650 029	108 577	Banana	42	1491	0.8	0.70
		8	650 001	108 554	Maize and banana	45	1471	0.42	1.10
	Deposition	9	649 939	108 625	Maize and banana	40	1462	0.6	0.92
		10	649 921	108 619	Coffee	33	1454	0.2	1.09
		11	649 985	108 510	Elephant grass	30	1464	0.24	1.03
		12	649 934	108 486	Banana	25	1438	1.22	0.71
Busiliwa	Head scarp	13	654 261	116 426	Coffee	54	1578	0.32	1.19
		14	654 267	116 410	Coffee	32	1571	0.24	1.12
		15	654 240	116 422	Abandoned	52	1581	0.03	0.75
		16	654 233	116 396	Coffee	50	1560	0.26	1.08
	Main body	17	654 281	116 395	Coffee and banana	47	1552	0.44	0.63
		18	654 286	116 369	Coffee	37	1549	0.14	0.38
		19	654 245	116 365	Banana	30	1543	0.18	0.54
		20	654 248	116 336	Coffee	26	1538	0.46	1.03
	Deposition	21	654 324	116 358	Banana and *sesbania*	35	1547	0.26	0.75
		22	654 333	116 339	Banana	45	1532	0.16	0.52
		23	654 258	116 323	Coffee	38	1537	0.36	0.65
		24	654 264	116 294	Coffee	43	1522	0.14	0.53
Bunakasala	Head scarp	25	653 495	117 304	Maize	32	1680	0.6	1.07
		26	653 485	117 302	Maize	42	1665	0.8	0.98
		27	653 492	117 330	Banana	52	1679	0.22	1.03
		28	653 476	117 338	Banana	38	1678	0.52	0.73
	Main body	29	653 450	117 377	Coffee	44	1660	0.32	0.53
		30	653 435	117 373	Cassava	33	1659	0.42	1.03
		31	653 448	117 282	Banana	48	1659	0.78	0.84
		32	653 426	117 279	Banana	53	1655	0.74	1.08
	Deposition	33	653 410	117 282	Banana	40	1644	0.32	0.80
		34	653 391	117 283	Banana	44	1640	0.38	0.83
		35	653 412	117 374	Elephant grass	43	1647	0.56	1.43
		36	653 398	117 376	Elephant grass	45	1640	0.44	1.20
Bunanyuma	Head scarp	37	647 019	116 906	Coffee	63	1789	1.10	0.90
		38	647 031	116 904	Coffee	59	1782	0.48	1.02
		39	647 049	116 959	Banana	51	1796	0.46	0.57
		40	647 061	116 944	Banana	59	1786	0.32	1.33
	Main body	41	647 046	116 900	Coffee	51	1774	0.09	1.29
		42	647 057	116 895	Coffee	46	1769	0.04	0.55
		43	647 073	116 943	Coffee	54	1778	0.62	1.28
		44	647 082	116 938	Coffee	56	1771	1.00	1.30
	Deposition	45	647 096	116 931	Banana	50	1763	0.76	1.23
		46	647 105	116 918	Banana	51	1758	0.82	0.94
		47	647 071	116 887	Banana	45	1766	0.40	1.18
		48	647 081	116 874	Banana	48	1764	0.58	1.25
Statistics for the measure of variation		Min				25	1438	0.03	0.38
		Max				63	1796	1.22	1.43
		Mean				44.8	1616.4	0.5	0.94
		Stdev				9.1	113.7	0.3	0.27
		CV (%)				20	7	63	29

CV = coefficient of variation; Stdev = standard deviation; Max = maximum; Min = minimum; Rpl = replicates.

lowest rate (0.4 cm/min) was observed in the main body section. The main body also depicted more variation than the other sections did. The coefficient of variation was 63%, 68%, and 62% for the head scarp, main body, and deposition section, respectively. When subjected to the ANOVA statistical test, the steady-state infiltration rates were not statistically different between the head scarp, main body, and deposition section (P value > 0.05). The

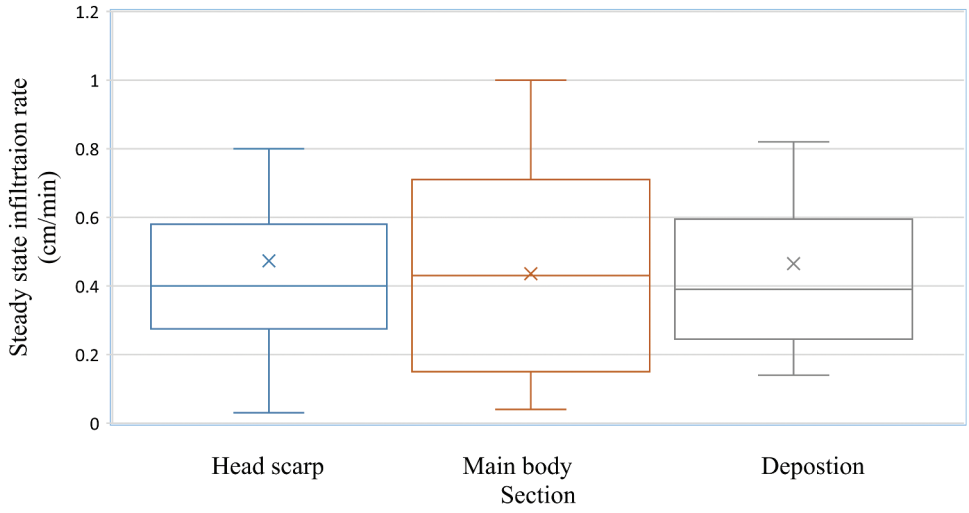

Figure 5. Variation of the steady-state infiltration rates across landslide scar sections for the entire catchment. The steady-state infiltration rate at the main body sections of the selected landslide scars depicted higher variation, followed by the deposition sections and then headscarp areas.

higher infiltration rate at the head scarp ignites rapid saturation of the pores, leading to increased pore pressure and mass weight. This elevated pore pressure then contributes to the detachment of mass from the bedrock and thus downslope movement. Furthermore, the intensified weight extends the fracturing process into the main body, perpetuating the land sliding process.

3.3.3 Saturated hydraulic conductivity between the studied landslide scars

Saturated hydraulic conductivity data within the catchment is presented in Table 6. The saturated hydraulic conductivity varied from 0.38 to 1.43 cm/min with an average of 1.04 cm/min. The average saturated hydraulic conductivity recorded was 0.94 cm/min, thus there was a high variation of the saturated hydraulic conductivity in the catchment (CV = 29%). The observed coefficient of variation is lower than 202.6% which was reported by Deb and Shukla (2012) for clay loam soils. The average saturated hydraulic conductivity (0.94 cm/min) is very rapid based on a categorization by Hazelton and Murphy (2007). The variation in the saturated hydraulic conductivity with study sites can be explained by the difference in land use, intrinsic soil properties, agricultural management, and climatic and environmental conditions at the sites (Deb and Shukla 2012, Muñoz *et al.* 2017).

3.3.4 Variation of soil-saturated hydraulic conductivity within the landslide scars

Results on the variation of saturated hydraulic conductivity among landslide scar sections in the catchment are presented in Fig. 6. At the head scarp, saturated hydraulic conductivity varied from 0.53 to 1.33 cm/min, thus averaging 0.97 cm/min. The main body recorded variation from 0.38 to 1.30 cm/min, averaging 0.92 cm/min. The saturated hydraulic conductivity in the deposition varied from 0.52 to 1.43 cm/min, averaging 0.94 cm/min. The coefficient of variation was 24%, 35%, and 29% for the head scarp, main body, and deposition section, respectively. The head scarp exhibited the highest saturated hydraulic conductivity, followed by deposition section and then the main body. There was no significant influence on saturated hydraulic conductivity by the landslide scar sections (P value > 0.05) of the studied area.

3.3.5 Statistical correlation between saturated hydraulic conductivity and steady-state infiltration rate within studied sites

The results of the correlation between saturated hydraulic conductivity and steady-state infiltration rates are summarized in Table 7. At Bunamungoma scar, there was a weak positive correlation (r^2 = 0.25, P = 0.44) between saturated hydraulic conductivity and steady-state infiltration rate. Saturated hydraulic conductivity at Busiliwa increased with an increase in the steady-state infiltration rate, exhibiting a moderate positive correlation (r^2 = 0.40, P = 0.20). Bunakasala site exhibited a weak positive correlation (r^2 = 0.24, P = 0.46). A very weak positive correlation (r^2 = 0.16, P = 0.62) was also recorded at Bunanyuma landslide scar. In summary, the hydraulic conductivity positively correlated with steady-state infiltration rate at all the studied landslide scar sites, though this correlation was not statistically significant.

4 Discussion

4.1 Variation of soil properties across the studied landslide scars

Across the study sites, both the steady infiltration rate and saturated hydraulic conductivity were high at the head scarp, followed by the deposition section, and then the main body. However, the variations were not significant, and this can be explained by limited variations within the soil physical properties. The level of soil organic matter in the head scarp could explain the higher steady infiltration rates, as the soils have limited capacity to hold water. Furthermore, the amount of bulk density (BD) could explain the increase in the infiltration rate and Ksat in the deposition section as there is less compaction of the soils, hence encouraging rapid water movement. According to Fuentes *et al.* (2004), Dec *et al.* (2008), and

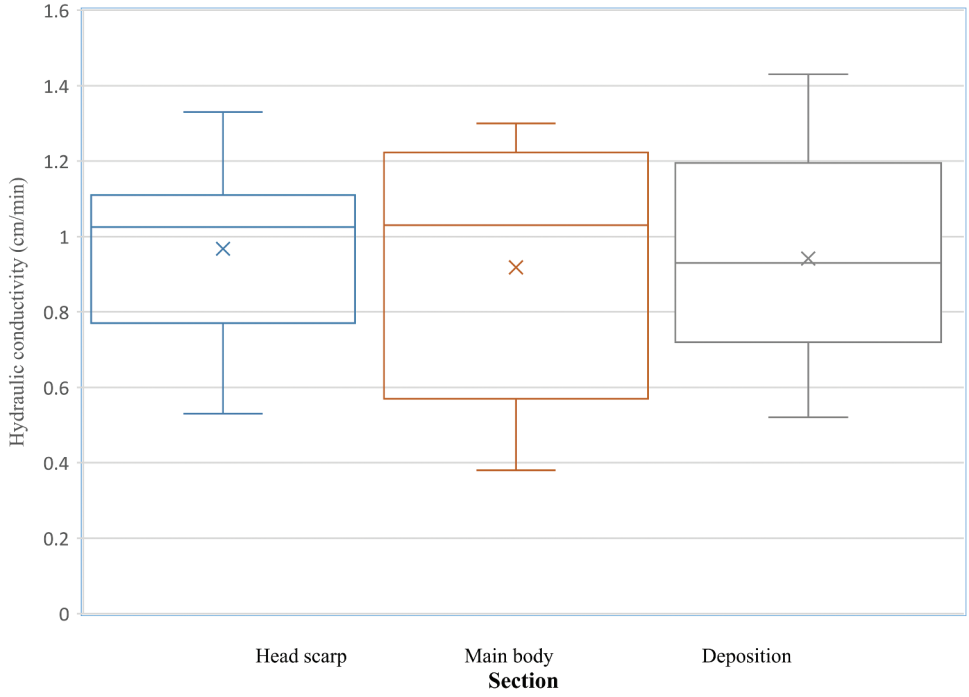

Figure 6. Variation of soil-saturated hydraulic conductivity across sections in the studied area. The main body sections of the chosen landslide scars exhibited the greatest variability in hydraulic conductivity, followed by the deposition sections and then the head scarp areas.

Table 7. Correlation between Ksat and steady-state infiltration rate.

No	Site	Correlation coefficient (r)	*P* value
1	Bunamungoma	0.57	0.05
2	Busiliwa	0.10	0.75
3	Bunakasala	0.46	0.13
4	Bunanyuma	0.04	0.91

Cleophas *et al.* (2022), an increase in bulk density leads to a reduction in macropores and an elevation in meso- and micropores, consequently influencing hydraulic conductivity.

4.2 Steady-state infiltration rate and saturated hydraulic conductivity

The observed steady-state infiltration rate (0.5 cm/min) at the studied sites is slightly higher than what Kitutu *et al.* (2009) recorded (0.45 cm/min) for the landslide-prone zones in Bududa district. However, the steady-state infiltration rates recorded at the landslide scar sites are far lower than those recorded in annual (1.81 cm/min) and perennial (1.95 cm/min) cropping systems on the volcanic sloping soils for the same area by Bamutaze *et al.* (2010). The variation in infiltration rates is attributed to the soil properties and land management practices at the study sites, which is consistent with studies by Chien-Yuan *et al.* (2005) and Meten *et al.* (2015).

Regarding catchments in other parts of the country, Kisira (2019), for instance, recorded an average infiltration of 0.35 cm/min on a hill slope of Kigezi highland, which is lower than observed for the studied landslide sites. This precisely explains the recurring landslides in Manafwa catchment with a higher level of infiltration in the Mount Elgon catchment. The average saturated hydraulic conductivity recorded (0.94 cm/min) was higher than (0.02 cm/min) that reported by Siriri *et al.* (2006), on different land use systems in Kigezi highlands. The high saturated hydraulic conductivity is due to the differences in land use practices as also noted by Siriri *et al.* (2006). The very rapid Ksat explains the increased susceptibility of Mount Elgon ecosystem to landslide disasters compared to other highlands in the country. The very rapid Ksat increases the steady-state infiltration rate in the head scarp as opposed to the main body which has shallow soil depth and an underlying bedrock that causes discontinuity in the vertical water movement in the soil. This is consistent with what was observed by Casagli *et al.* (2006) and Gomes and Vieira (2004). More literature indicates that saturated hydraulic conductivity influences the rate of water movement in the soil (Duan *et al.* 2018, Soulis *et al.* 2020). The very rapid Ksat increases the water pore pressure in the head scarp thus reducing the soil stability that initiates land sliding.

4.3 Effect of soil physical properties on infiltration rate and saturated hydraulic conductivity

Soil textural class and bulk density significantly influenced infiltration and saturated hydraulic conductivity which triggered landslides at the studied scar sites. The high clay content in the soils and its influence on landslide occurrence in Manafwa catchment is not surprising. Kitutu *et al.* (2009) obtained similar results and noted that soil texture at different soil depths was significant in triggering some landslides. In addition, Mugagga *et al.* (2012a) stated that if soils have > 32% clay this implies tremendous slumping potential and thus high susceptibility to landslides. In a study elsewhere, Turk (2017) comments on the effect of soil properties on landslides along forest roads and reveals that soils dominated by clay loams are

more susceptible to landslides due to the high spreading rate. For soil management purposes, the high clay content implies that there is a need to apply soil and water conservation practices that increase humus such as applying organic compost manure. This improves the soil structure and eliminates drainage and compaction problems, as revealed by Eberbach and Humphreys (2014).

The average of 1.26 g/cm^3 showed low BD composition, below the critical level of 1.6 g/cm^3 for clay loam as advanced by Hazelton and Murphy (2007). This therefore increases the volumetric air content in the soil as well as easily allowing root penetration, as also observed by Field. Bulk density in the studied sites was low, thus increasing saturated hydraulic conductivity and infiltration rate (Igwe 2005). Similar results have been reported in other catchments. For example, Fonseca and Lani (2017) revealed that low bulk density increases saturated hydraulic conductivity and total porosity provides more space for water which enhances soil saturation and landslide occurrence. Low bulk density decreases overland flow by increasing the infiltration (Efthimiou 2019). Practices like the use of multicrop systems with different rooting depths and no-tillage cropping systems improve bulk density (USDA NRCS 2019).

The observed soil organic matter level was below the critical level of 3% (Okalebo *et al.* 2002). Soil organic matter controls water infiltration, transmission, and storage in the soil (Franzluebbers 2002). Reduced soil organic matter therefore implies that there is un-controlled increase of water infiltration, thus causing soil pores to fill very fast. Continued infiltration increases water pore pressure, increasing the susceptibility of slopes to slide. Soil organic matter can be improved through good practices, for instance reduction of erosion through mulching, minimum tillage, and planting of cover crops or high residue crops (Cotrufo and Lavallee, 2021).

5 Conclusions

In general, the results of this study demonstrate that the medium landslide scars in the Manafwa catchment are characterized by high and very rapid steady-state infiltration rates and saturated hydraulic conductivity. The steady-state infiltration rate is generally high across the scar sections but relatively higher at the head scarp section, which serves as the initiation point for landslides in such areas. The organic matter content was low in the upper and lower soil depth, unlike the clay content which was high and increased with soil depth. Practices such as the application of organic fertilizers that increase soil organic matter should be promoted to enhance soil stability.

Acknowledgements

The first author gratefully acknowledges Water, Society, and Climate Change (WaSo) for their partial financial support towards this research.

Disclosure statement

No potential conflict of interest was reported by the author(s).

Funding

This work was funded by Norwegian Agency for Development Cooperation through the Water and Society (WASO) Project Makerere University, Kampala, Uganda.

ORCID

Moses Kutosi http://orcid.org/0009-0003-9288-034X
Yazidhi Bamutaze http://orcid.org/0000-0003-1744-9827
Bob R. Nakileza http://orcid.org/0000-0002-9718-0460
Yeeko Kisira http://orcid.org/0000-0001-8072-6781
Geofrey Gabiri http://orcid.org/0000-0002-7200-7717

Data availability statement

The data belongs to the project and will be shared by the corresponding author on request.

References

Acaps, 2018. *Flooding and landslides in Bududa district*. https://reliefweb.int/sites/reliefweb.int/files/resources/20181018_acaps_start_briefing_note_uganda_flooding_and_landslides_in_bududa.pdf.

Amoozegar, A. and Wilson, G.V., 1999. Methods for measuring hydraulic conductivity and drainable porosity. *Agronomy Monograph*, 38, 1149–1205. doi:10.2134/agronmonogr38.c37.

Aristizábal, E., Vélez, J.I., and Martínez, H., 2016. Influences of antecedent rainfall and hydraulic conductivity on landslides triggered by rainfall occurrence using the model Shia_Landslide. *Revista EIA*, 13 (26), 31–36. doi:10.24050/reia.v13i26.863.

Bamutaze, Y., *et al.* 2010. Infiltration characteristics of volcanic sloping soils on Mt. Elgon, Eastern Uganda. *Catena*, 80 (2), 122–130. doi:10.1016/j.catena.2009.09.006.

Bamutaze, Y., 2019. Morphometric conditions underpinning the spatial and temporal dynamics of landslide hazards on the volcanics of Mt. Elgon, Eastern Uganda. *In*: F. I. Rivera, ed. *Emerging voices in natural hazards research*. Elsevier, 57–81. doi:10.1016/B978-0-12-815821-0.00010-2.

Bicocchi, G., *et al.* 2019. Geotechnical and hydrological characterization of hillslope deposits for regional landslide prediction modeling. *Bulletin of Engineering Geology and the Environment*, 78 (7), 4875–4891. doi:10.1007/s10064-018-01449-z.

Bogaard, T. and Greco, R., 2014. Preface "Hillslope hydrological modelling for landslides prediction." *Hydrology and Earth System Sciences*, 18, 4185–4188. doi:10.5194/hess-18-4185-2014.

Bouwer, H., 1986. Intake rate: cylinder infiltrometer. *Methods of Soil Analysis: Part 1 Physical and Mineralogical Methods*, 5, 825–844. doi:10.2136/sssabookser5.1.2ed.c32.

Broeckx, J., *et al.* 2018. Landslide susceptibility and mobilization rates in the Mount Elgon region, Uganda. *Landslides*. doi:10.1007/s10346-018-1085-y.

Brouwer, C., *et al.* 1988. Irrigation water management: irrigation methods. *Training Manual*, 9 (5), 5–7. http://soilhealth.ucdavis.edu/application/files/2815/4208/2325/Irrigation_Water_Management.pdf.

Casagli, N., *et al.* 2006. Analysis of the landslide triggering mechanism during the storm of 20th – 21st November 2000, in Northern Tuscany. Landslides, 3 (1), 13–21. doi:10.1007/s10346-005-0007-y.

Chien-Yuan, C., *et al.* 2005. Analysis of time-varying rainfall infiltration induced landslide. *Environmental Geology*, 48 (4–5), 466–479. doi:10.1007/s00254-005-1289-z.

Chien-yuan, C. and Tien-chien, C., 2017. Analysis of time-varying rainfall infiltration induced landslide. August 2005. *Environmental Geology*. doi:10.1007/s00254-005-1289-z.

Chiu, Y.Y., Chen, H.E., and Yeh, K.C., 2019. Investigation of the influence of rainfall-runoff on shallow landslides in unsaturated soil using a mathematical model. *Water (Switzerland)*, 11 (6). doi:10.3390/w11061178.

Cho, S.E., 2014. Probabilistic stability analysis of rainfall-induced landslides considering spatial variability of permeability. *Engineering Geology*, 171 (2014), 11–20. doi:10.1016/j.enggeo.2013.12.015.

Cho, S.E., 2017. Prediction of shallow landslide by surficial stability analysis considering rainfall infiltration. *Engineering Geology*, 231, 126–138. doi:10.1016/j.enggeo.2017.10.018.

Cleophas, F., *et al*. 2022. Effect of soil physical properties on soil infiltration rates. *Journal of Physics: Conference Series*, 2314 (1), 12020. doi:10.1088/1742-6596/2314/1/012020.

Cotrufo, M.F. and Lavallee, J.M., 2021. Soil organic matter formation, persistence, and functioning: a synthesis of current understanding to inform its conservation and regeneration. *Advances in Agronomy*, 172, 1–66. doi:10.1016/bs.agron.2021.11.002.

Couto, M.F., Peternelli, L.A., and Barbosa, M.H.P., 2017. Classification of the coefficients of variation for sugarcane crops. *Ciência Rural*, 43 (6), 957–961. doi:10.1590/s0103-84782013000600003.

Deb, S.K. and Shukla, M.K., 2012. Variability of hydraulic conductivity due to multiple factors. *American Journal of Environmental Sciences*, 8 (5), 489–502. doi:10.3844/ajessp.2012.489.502.

Dec, D. *et al.*, 2008. Effect of bulk density on hydraulic properties of homogenized and structured soils. *Journal of Soil Science and Plant Nutrition*, 8 (1).

Dick, R.P., Thomas, D.R., and Halvorson, J.J., 2015. Standardized methods, sampling, and sample pretreatment. *Methods for Assessing Soil Quality*, 107–121. doi:10.2136/sssaspecpub49.c6.

Dörner, J., *et al*. 2022. Short-term effects of compaction on soil mechanical properties and pore functions of an Andisol. *Soil and Tillage Research*, 221, 105396. doi:10.1016/j.still.2022.105396.

Duan, X., *et al*. 2018. Variation in soil-saturated hydraulic conductivity along the hillslope of collapsing granite gullies. *Hydrological Sciences Journal*, 63 (5), 803–817. doi:10.1080/02626667.2018.1453610.

Duan, Z., *et al*. 2023. Mechanical and microscopic properties of soil according to the rate of increase in pore water pressure. *Soil and Tillage Research*, 225, 105530. doi:10.1016/j.still.2022.105530.

Eberbach, P.L., and Humphreys, E., 2014. Simulation of the evaporation of soil water beneath a wheat crop canopy. *Agricultural Water Management*, 135, 19–26. doi:10.1016/j.agwat.2013.12.008.

Efthimiou, N., 2019. Development and testing of the Revised Morgan-Morgan-Finney (RMMF) soil erosion model under different pedological datasets erosion model under di ff erent pedological datasets. *Hydrological Sciences Journal*, 64 (9), 1095–1116. doi:10.1080/02626667.2019.1623896.

Fonseca, L.D.M. and Lani, J.L., 2017. Variabilidade dos atributos físicos do solo em áreas suscetíveis ao deslizamento de terra. *Acta Scientiarum - Agronomy*, 39 (1), 109–118. doi:10.4025/actasciagron.v39i1.30561.

Franzluebbers, A.J., 2002. Water infiltration and soil structure related to organic matter and its stratification with depth. *Soil and Tillage Research*, 66 (2), 197–205. doi:10.1016/S0167-1987(02)00027-2.

Fuentes, J.P., Flury, M., and Bezdicek, D.F., 2004. Hydraulic properties in a silt loam soil under natural prairie, conventional till, and No-till. *Soil Science Society of America Journal*, 68 (5), 1679–1688. doi:10.2136/sssaj2004.1679.

Galeandro, A., *et al*. 2014. Analysis of infiltration processes into fractured and swelling soils as triggering factors of landslides. *Environmental Earth Sciences*, 71 (6), 2911–2923. doi:10.1007/s12665-013-2666-7.

Gomes, R.A.T. and Vieira, B.C., 2004. Landslides in Rio de Janeiro : the role played by variations in Topographic controls of landslides in Rio de Janeiro : field evidence and modeling. *Hydrological Processes*, 2017. doi:10.1002/hyp.1363.

Guo, Y. and Ma, C., 2023. Elucidating the role of soil hydraulic properties on aspect-dependent landslide initiation. *Hydrology and Earth System Sciences*, 27 (8), 1667–1682. doi:10.5194/hess-27-1667-2023.

Guzzetti, F., *et al*. 2012. Landslide inventory maps: new tools for an old problem. *Earth-Science Reviews*, 112 (1–2), 42–66. doi:10.1016/j.earscirev.2012.02.001.

Hazelton, P. and Murphy, B., 2007. Interpreting Soil Test Results: what do all the Numbers mean? - by P. Hazelton & B.Murphy. *European Journal of Soil Science*, 58 (5), 1219–1220. doi:10.1111/j.1365-2389.2007.00943_8.x.

Hiramatsu, S., *et al*. 1993. Study for prediction of occurrence of hillside landslides. IAHS PUBLICATION, 75. https://iahs.info/uploads/dms/9506.75-81-217-Hiramatsu.pdf.

Huang, F., *et al*. 2022. Influence of heavy rainfall and different slope cutting conditions on stability changes in red clay slopes: a case study in South China. *Environmental Earth Sciences*, 81 (15), 384. doi:10.1007/s12665-022-10466-x.

Igwe, C.A., 2005. Soil physical properties under different management systems and organic matter effects on soil moisture along soil catena in southeastern Nigeria. *Tropical and Subtropical Agroecosystems*, 5 (2), 57–66. https://www.redalyc.org/pdf/939/93950202.pdf.

James, D.W. and Wells, K.L., 2018. Soil sample collection and handling: technique based on source and degree of field variability. *Soil Testing and Plant Analysis*, 3, 25–44. doi:10.2136/sssabookser3.3ed.c3.

Kervyn, M., *et al*. 2015. Landslide resilience in Equatorial Africa: moving beyond problem identification. *Belgeo*, 1 (2015), 1–19. doi:10.4000/belgeo.15944.

Kisira, Y., 2019. *Patterns of infiltration on a bench terraced hillslope of Kigezi highlands*. Master's dissertation. Makerere University. http://hdl.handle.net/10570/7766.

Kisira, Y., *et al*. 2022. Persons with disabilities and resilience: coping with environmental hazards case of landslides in Mount Elgon region, Uganda. *Environmental Hazards*, 1–18. doi:10.1080/17477891.2022.2149454.

Kitutu, K.M.G., 2010. *Landslide occurrences in the hilly areas of Bududa District in Eastern Uganda and their causes*. Doctoral dissertation. Makerere University. http://hdl.handle.net/10570/2246 .

Kitutu, M.G., *et al*. 2009. Influence of soil properties on landslide occurrences in Bududa district, Eastern Uganda. *African Journal of Agricultural Research*, 4 (July), 611–620. doi:10.5897/AJAR09.158.

Lora, M., *et al*. 2016. Rainfall-triggered shallow landslides: infiltration dynamics in a physical hillslope model. *Hydrological Processes*, 30 (18), 3239–3251. doi:10.1002/hyp.10829.

Meten, M., PrakashBhandary, N., and Yatabe, R., 2015. Effect of landslide factor combinations on the prediction accuracy of landslide susceptibility maps in the Blue Nile Gorge of Central Ethiopia. *Geoenvironmental Disasters*, 2 (1). doi:10.1186/s40677-015-0016-7.

Mugagga, F., Kakembo, V., and Buyinza, M., 2012a. A characterisation of the physical properties of soil and the implications for landslide occurrence on the slopes of Mount Elgon, Eastern Uganda. *Natural Hazards*, 60 (3), 1113–1131. doi:10.1007/s11069-011-9896-3.

Mugagga, F., Kakembo, V., and Buyinza, M., 2012b. Land use changes on the slopes of Mount Elgon and the implications for the occurrence of landslides. *Catena*, 90 (March), 39–46. doi:10.1016/j.catena.2011.11.004.

Muñoz, D.R., *et al*. 2017. Analyzing the effect of land use and vegetation cover on soil infiltration in three contrasting environments in northeast Spain. *Cuadernos de investigación geográfica: Geographical Research Letters*, 43 (1), 141–169. https://dialnet.unirioja.es/servlet/articulo?codigo=6126654.

Nakileza, B.R., *et al*. 2017. Enhancing resilience to landslide disaster risks through rehabilitation of slide scars by local communities in Mt Elgon, Uganda. *Jàmbá: Journal of Disaster Risk Studies*, 9 (1), 1–11. doi:10.4102/jamba.v9i1.390.

Nakileza, B.R. and Nedala, S., 2020. Topographic influence on landslides characteristics and implication for risk management in upper Manafwa catchment, Mt Elgon Uganda. *Geoenvironmental Disasters*, 7 (27), 1–13. doi:10.1186/s40677-020-00160-0.

Okalebo, J.R., Gathua, K.W., and Woomer, P.L., 2002. Laboratory methods of soil and plant analysis: a working manual second edition. *Sacred Africa, Nairobi*, 21, 25–26. https://www.researchgate.net/profile/Dilip-Kundu/post/Which-is-accurate-way-for-measuring-P-content/attachment/59d6455d79197b80779a07dc/AS%3A452837697167361%401484976328229/download/Soil+Analyses+manual.pdf.

Osuret, J., *et al*. 2016. Coping Strategies for Landslide and Flood Disasters: a Qualitative Study of Mt. Elgon Region, Uganda. *PLOS Currents* 8. doi:10.1371/currents.dis.4250a225860babf3601a18e33e172d8b.

Perkins, L.B., *et al*. 2013. Quick start guide to soil methods for ecologists. *Perspectives in Plant Ecology, Evolution and Systematics*, 15 (4), 237–244. doi:10.1016/j.ppees.2013.05.004.

Petley, D., 2012. Global patterns of loss of life from landslides. *Geology*, 40 (10), 927–930. doi:10.1130/G33217.1.

Qin, M., *et al*. 2022. Occurrence of shallow landslides triggered by increased hydraulic conductivity due to tree roots. *Landslides*, 19 (11), 2593–2604. doi:10.1007/s10346-022-01921-8.

Samara, E., Matsi, T., and Balidakis, A., 2017. Soil application of sewage sludge stabilized with steelmaking slag and its effect on soil properties and wheat growth. *Waste Management*, 68, 378–387. doi:10.1016/j.wasman.2017.06.016.

Singh, R.G., *et al*. 2008. Holocene landslides in KwaZulu-Natal South Africa. *South African Journal of Geology*, 111 (1), 39–52. doi:10.2113/gssajg.111.1.39.

Siriri, D., *et al*. 2006. Water infiltration, conductivity and runoff under fallow agroforestry on sloping terraces. *African Crop Science Journal*, 14 (1), 59–71. https://www.ajol.info/index.php/acsj/article/view/135851/125347.

Soulis, K.X., Londra, P.A., and Kargas, G., 2020. Characterizing surface soil layer saturated hydraulic conductivity in a Mediterranean natural watershed. *Hydrological Sciences Journal*, 65 (15), 2616–2629. doi:10.1080/02626667.2020.1831694.

Tamale, J., 2014. *Soil characterization in the landslide-prone area Bumwalukani, Eastern Uganda*. Doctoral dissertation. Vrije Universiteit Brussel Belgium. https://libstore.ugent.be/fulltxt/RUG01/002/166/738/RUG01-002166738_2014_0001_AC.pdf.

Tian, W., *et al*. 2022. Slope stability analysis method of unsaturated soil slopes considering pore gas pressure caused by rainfall infiltration. *Applied Sciences*, 12 (21), 11060. *Applied Sciences (Switzerland), 12* (21). doi:10.3390/app122111060.

Travelletti, J., *et al*. 2011. Hydrological response of weathered clay-shale slopes : water infiltration monitoring with time-lapse electrical resistivity tomography. *Hydrological Processes*. doi:10.1002/hyp.7983.

Turk, Y., 2017. The effect of soil properties on landslides along Forest Road the effect of soil properties on landslides along Forest Road. *European Journal of Forest Engineering*, 3 (1), 1–7.

USDA NRCS. (2019, May). Soil health-guides for educators: soil bulk density/moisture/aeration. United States department of agriculture - natural resources conservation service. *Soil Quality Kit-Guides for Educators*, 1–11. https://www.nrcs.usda.gov/wps/portal/nrcs/detailfull/soils/health/assessment/?cid=nrcs142p2_053870.

Wayllace, A., *et al*. 2019. Hydrological behavior of an infiltration-induced landslide in Colorado, USA. *Geofluids*, 2019, 1–14. doi:10.1155/2019/1659303.

Wodeya, D., 2018. *Effects of land use/cover change on hydrological flow of river Manafwa, Uganda*. Masters dissertation. http://hdl.handle.net/10570/7064.

Yeh, H.F. and Tsai, Y.J., 2018. Analyzing the effect of soil hydraulic conductivity anisotropy on slope stability using a coupled hydromechanical framework. *Water (Switzerland)*, 10 (7), 905. doi:10.3390/w10070905.

Yimer, F., Alemu, G., and Abdelkadir, A., 2015. Soil property variations in relation to exclosure and open grazing land use types in the Central Rift Valley area of Ethiopia. *Environmental Systems Research*, 4 (1). doi:10.1186/s40068-015-0041-2.

Zhang, H., *et al*. 2020. Spatial distribution of soil organic matter in a coal mining subsidence area. *Acta Agriculturae Scandinavica Section B: Soil and Plant Science*, 70 (2), 117–127. doi:10.1080/09064710.2019.1676916.

Zhang, Z., *et al*. 2023. Effects of changes in soil properties caused by progressive infiltration of rainwater on rainfall-induced landslides. *Catena*, 233 (December), 1–6. doi:10.1016/j.catena.2023.107475.